

The fission barriers in Actinides and superheavy nuclei in covariant density functional theory

S. Karatzikos¹, A. V. Afanasjev², G. A. Lalazissis¹, P. Ring³

¹ Department of Theoretical Physics, Aristotle University of Thessaloniki GR-54006, Thessaloniki, Greece

² Department of Physics and Astronomy, Mississippi State University, Mississippi State, Mississippi 39762, USA

³ Physik-Department, Technische Universität München D-85747, Garching, Germany

Abstract

The impact of pairing correlations on the fission barriers is investigated in Relativistic Hartree Bogoliubov (RHB) theory and Relativistic Mean Field (RMF)+BCS calculations. It is concluded that the constant gap approximation in the usual RMF+BCS calculations does not provide an adequate description of the barriers. The RHB calculations show that there is a substantial difference in the predicted barrier heights between zero-range and finite range pairing forces even in the case when the pairing strengths of these two forces are adjusted to the same value of the pairing gap at the ground state.

Key words: Fission barrier, covariant density functional theory, pairing

PACS: 21.60.Jz, 24.75.+i, 25.85.CA, 25.85.-w

1. Introduction

A study of the (static) fission-barrier height B_f^{st} of nuclei is motivated by the importance of this quantity for several physical phenomena. Many heavy nuclei decay by spontaneous fission, and the size of the fission barrier is a measure of stability of the nucleus reflected in the spontaneous fission lifetimes of these nuclei [1]. The probability for the formation of a superheavy nucleus in a heavy-ion-fusion reaction is also directly connected to the height of its fission barrier [2]. The height B_f^{st} is a decisive quantity in the competition between neutron evaporation and fission of a compound nucleus in the process of its cooling. The large sensitivity of the cross section σ for the synthesis of the fissioning nuclei on the barrier height B_f^{st} stresses a need for accurate calculations of this value. For example, a change of B_f^{st} by 1 MeV changes the calculated survival probability of a synthesized nucleus by about one order of magnitude or even more [2]. The population and survival of hyperdeformed states at high spin also depends on the fission barriers, see e.g. Refs. [3, 4]. In addition, the r -process of stellar nucleosynthesis depends (among other quantities such as masses and β -decay rates) on the fission barriers of very neutron-rich nuclei [5, 6].

The fission barriers for Actinides and super-heavy nuclei show significant differences when calculated by various theoretical approaches (see, for example, Fig. 25 in Ref. [1] and Fig. 2 in Ref. [2]). Many extensive calculations of fission barriers have been done in the framework of the macroscopic+microscopic (MM) method (see Refs. [7, 8, 9, 10, 11, 12] and references therein). In addition, after the pioneering work of Flocard et al. [13] a growing number of self-consistent investigations have been reported in recent years. These calcu-

lations are based on modern energy density functionals. After semiclassical investigations [14] there are now fully quantum mechanical calculations available based on Skyrme [15, 16, 17, 18, 19, 20], Gogny [21, 22] or RMF [23, 24, 16, 4] functionals. The majority of these calculations are restricted to axially symmetric shapes. In reality, however, the axially symmetric fission barriers sometimes indicate only an upper limit, because calculations including triaxiality [20, 25, 22, 15] have found a lowering of the fission barrier by up to several MeV. This lowering strongly depends on the proton and neutron number and on the model employed.

So far all investigations of fission barriers based on covariant density functional theory (CDFT) have been performed in the RMF+BCS framework [24, 15, 17]. One of the major goals of the current manuscript is to perform the detailed comparative study of the inner fission barriers in the RMF+BCS and in the relativistic Hartree-Bogoliubov (RHB) frameworks. In particular, we try to understand to what extent the properties of the first barrier are influenced by the impact of different pairing schemes and how the uncertainties in the extrapolation of the pairing strength towards super-heavy region affect the fission barriers in these nuclei. In order to save computational time we do not consider the outer fission barriers in the current investigation. This restriction has its own merits. The inner barriers are generally better measured than the outer ones, and they are certainly more important for the r -process, since they determine the thresholds. Furthermore, spontaneous fission lifetimes tend to be dominated by the inner barrier, even if occasionally an outer barrier can have a crucial effect if it is large enough. The consideration of only inner fission barriers allows us to restrict the calculations to reflection symmetric shapes, because it has

been found in several investigations [24, 20, 19, 25, 18] that odd-multipole deformations (octupole, etc.) do not play a role in the inner fission barrier of the Actinides and of superheavy nuclei.

The manuscript is organized as follows. The theoretical framework, the selection of pairing schemes and the numerical details of calculations are discussed in Sect. 2. In Sect. 3 we study the influence of pairing correlations on the shape and the height of the inner fission barrier. Experimental data on fission barriers in Actinides and superheavy nuclei is compared with the results of such calculations in Sect. 4. Finally, Sect. 5 contains the main conclusions of our work.

2. Theoretical framework and numerical details

The calculations discussed in the current manuscript are based on two mean field methods to treat pairing correlations in nuclei:

2.1. RMF+BCS calculations

The RMF+BCS scheme is rather simple. The RMF-equations are solved and at each step of the iteration the BCS occupation probabilities v_k^2 are determined. These quantities are used in the calculation of densities, energies and new fields for the next step of the iteration. Two methods are available for the evaluation of the occupation numbers v_k^2 , either the "constant gap" approximation [26, 27] or the solution of the gap equations based on a seniority force with the strength parameters G_τ for neutrons ($\tau = n$) and protons ($\tau = p$) (denoted in the following "constant G ").

In the first case (constant gap) one starts with fixed gap parameters Δ and uses the BCS expression

$$v_k^2 = \frac{1}{2} \left(1 - \frac{\varepsilon_k - \lambda}{E_k} \right) \quad (1)$$

with $E_k = \sqrt{(\varepsilon_k - \lambda)^2 + \Delta^2}$ for the occupation numbers and for the pairing energy

$$E_{\text{pair}} = -\Delta \sum_{k>0} u_k v_k \quad (2)$$

ε_k are the eigenvalues of the Dirac equation and the chemical potentials λ are determined by the particle numbers.

In the second case (constant G) one starts with pairing strengths parameters G and solves in each step of the iteration the gap equation [28]

$$\frac{1}{G} = \sum_{k>0} \frac{1}{2E_k} \quad (3)$$

and determines the gap parameters

$$\Delta = G \sum_{k>0} u_k v_k \quad (4)$$

in a self-consistent way. This method is based on the residual interaction of the seniority model [28] and its strength parameters G .

In principle both methods are equivalent if the constants G are adjusted properly to the corresponding gap parameters Δ (or vice versa). There is, however a difference between the two models when we carry out calculations along the fission path by constraining the deformation. In the first case (constant gap) the gap parameters Δ are kept fixed as a function of the deformation. This means the equivalent strength parameters G change with deformation. In the second case (constant G) we use a fixed pairing force with constant strength parameters G for all deformations and the gap parameters Δ change with deformation. This situation is, of course, closer to reality.

2.2. Fully self-consistent RHB calculations

The second method used in this investigation is based on a fully self-consistent solution of the relativistic Hartree-Bogoliubov (RHB) equations as introduced in Refs. [29, 30]:

$$\begin{pmatrix} h_D - \lambda & \Delta \\ -\Delta^* & -h_D^* + \lambda \end{pmatrix} \begin{pmatrix} U \\ V \end{pmatrix}_k = E_k \begin{pmatrix} U \\ V \end{pmatrix}_k \quad (5)$$

where h_D is the Dirac hamiltonian of RMF-theory and the pairing field

$$\Delta_{12} = \sum_{3<4} V_{1234}^{\text{pp}} \kappa_{34} \quad (6)$$

is determined in a self-consistent way by the pairing tensor

$$\kappa_{12} = \sum_k V_{2k}^* U_{1k}, \quad (7)$$

and an effective pairing interaction V^{pp} . The pairing energy is given by

$$E_{\text{pair}} = -\frac{1}{2} \text{Tr} \Delta \kappa. \quad (8)$$

In the present investigations we compare two different pairing interactions. First we use the Brink-Booker part of the Gogny force with finite range

$$V^{\text{pp}}(1, 2) = \sum_{i=1,2} e^{-(r/\mu_i)^2} (W_i + B_i P^\sigma - H_i P^\tau - M_i P^\sigma P^\tau), \quad (9)$$

where P^σ and P^τ are the exchange operators for spin and isospin and the parameters μ_i , W_i , B_i , H_i , and M_i ($i = 1, 2$) of this force have been carefully adjusted to the G-matrix calculations in nuclear matter and to the pairing properties of finite nuclei all over the periodic table (for details of this fit see Refs. [31, 32]). We use here the parameter set D1S [21].

As second example we use a zero range δ -force

$$V^{\text{pp}}(1, 2) = -V_0 \delta(\mathbf{r}_1 - \mathbf{r}_2), \quad (10)$$

as it has been used in many non-relativistic HFB calculations [18]. This interaction does not depend on density and thus it leads to volume pairing.

In RHB-calculations the pairing gap of BCS-theory is replaced by the pairing field Δ_{12} in Eq. (6). In order to have a simple measure for the size of pairing correlations in RHB

theory we therefore introduce in the following calculations the "average gap" in the canonical basis

$$\langle \Delta \rangle = \frac{\sum_k v_k^2 \Delta_{k\bar{k}}}{\sum_k v_k^2} \quad (11)$$

where v_k^2 are the eigenvalues of the density matrix $\rho_{12} = \sum_k V_{2k}^* V_{1k}$ in the canonical basis and $\Delta_{k\bar{k}}$ are the diagonal matrix elements of the pairing field Δ in this basis. For details see Ref. [28]

2.3. The pairing window

Pairing is restricted to the vicinity of the Fermi surface and the size of this vicinity is essentially characterized by the gap parameter Δ . This parameter determines the distribution of occupations numbers v_k^2 and therefore most of the experimental quantities depending on pairing correlations. Of course, in BCS or HFB theory based on the seniority model or on zero range forces the sums in Eqs. (2,3,4, or 7) show an ultra-violet divergence and one has to limit the sums in Eqs. (2,3,4) to a pairing window $\varepsilon_k < E_{\text{cut-off}}$ and in Eq. (7) to $E_k < E_{\text{cut-off}}$. Concerning this pairing window, there is a difference between the methods of constant gap and constant G . In the method of constant gap, the essential quantity Δ is fixed and determined in one or another way by experiment. The size of the pairing window enters only in the calculation of the pairing energy (2) which is not measurable. For reasonable pairing windows the pairing energy is small as compared to the binding energy of the system and by this reason one often finds the remark in the literature that the results do not depend on the pairing window. However, the situation is different for the method of constant G or for zero range forces. In this case the size of the effective pairing constants G or V_0 in Eq. (10) have to be adjusted in such a way, that the resulting gap parameters Δ correspond roughly to the experimental gaps. As a consequence there is a strong connection between the strength of the pairing force and the cut-off energy $E_{\text{cut-off}}$. It makes no sense to give only the strength parameter G (or V_0) if the corresponding value of $E_{\text{cut-off}}$ is not known. Essentially one is left with the problem that one has one experimental quantity Δ and two unknowns G (or V_0) and $E_{\text{cut-off}}$. Usually one chooses a fixed value for $E_{\text{cut-off}}$ in a somewhat arbitrary way and determines the corresponding strength parameters in such way that the gap parameter Δ corresponds more or less to the experimental value.

Bulgac [33] has proposed an elegant way to regularize the divergence of the gap equation in r -space by removing the divergent part of the pairing tensor (7) producing in this way a zero-range pairing force, which depends only on one parameter. On the other side, as it is clearly seen in momentum space, the two parameters G (or V_0) and $E_{\text{cut-off}}$ are connected to two different physical quantities, namely, to the strength and the range of the effective pairing force. This means that $E_{\text{cut-off}}$ should not be chosen in an arbitrary way, but it should be determined by the range of the force. Of course, it not clear which experimental quantity is really sensitive to the range of the effective pairing force. To search for such quantities one could do calculations

with finite range pairing forces of different range adjusting in each case the remaining parameters to the experimental gap. In this context we will study in Sect. 3 the influence of the pairing window of zero-range pairing forces on the size of the fission barriers.

Gogny [31, 34] has avoided the problem of the pairing window by using a finite range force of Gaussian type where the range is adjusted to a G -matrix, i.e. via an ab-initio calculation directly to the properties of the bare nucleon-nucleon interaction. The fact that this pairing force is extremely successful in reproducing an astonishing number of experimental data both in non-relativistic [31, 35, 36] and relativistic energy density functionals [37, 38, 39] shows that this choice of the range is deeply connected to the physics of the nuclear many-body problem.

2.4. Numerical details

In the current manuscript, we use new versions of the RMF+BCS and RHB codes which were specifically designed to describe axially symmetric nuclei with large elongation. They allow to use different numbers of integration points in the directions along the symmetry axis and in perpendicular direction thus allowing a better numerical description of highly elongated systems. As discussed in Refs. [27, 40] the RMF+BCS and RHB equations are solved in the basis of an axially deformed harmonic oscillator potential characterized by the deformation parameter β_0 and oscillator frequency $\hbar\omega_0 = 41A^{-1/3}$ MeV. The truncation of basis is performed in such a way that all states belonging to the shells up to N_F fermionic shells and N_B bosonic shells are taken into account. The computational time increases considerably with the increase of N_F but it is much less dependent on N_B . Thus, a special attention has been paid to the selection of N_F of the basis which would allow for a systematic study of fission barriers in the nuclei of interest, providing at the same time a reasonable numerical accuracy in the predictions of the physical observables.

Extensive tests of numerical convergence have been performed in the spherical, normal-deformed and superdeformed ($\beta_2 \sim 0.7-1.0$) minima in the RMF calculations without pairing on the example of the nuclei ^{238}U and $^{304}120$ with $Z = 120$ and $N = 184$. Contrary to the previous studies of the convergence in the RMF framework which were based on the comparison of the N_F and $N_F + 2$ results, we first defined the "exact" solution (extending the calculations up to $N_F = 36$, $N_B = 36$) which does not change with the increase of N_F , and then found the truncation scheme for a basis which provides sufficient numerical accuracy. It turns out that the binding energies for $N_F = 20$ and $N_B = 20$ are described with an accuracy of 200 keV as compared with the exact solution. It was also checked that the inner fission barrier is described with an accuracy of ~ 100 keV both in the RMF+BCS and RHB calculations in this truncation scheme. Thus all the following calculations are performed with $N_F = N_B = 20$.

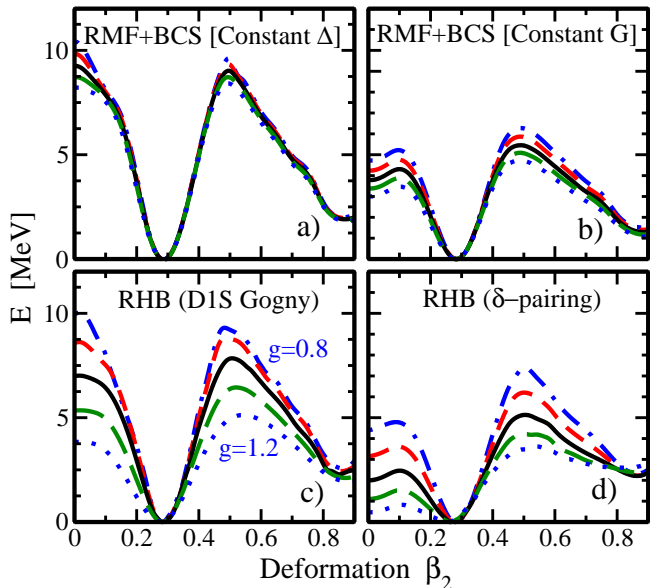


Figure 1: (Color online) Potential energy surfaces in ^{240}Pu obtained in different pairing schemes with the NL3 parameterization of the RMF Lagrangian and different values of the scaling factor g . They are normalized to the energy of the normal-deformed (ND) minimum. Further details are given in the text.

3. The role of pairing in defining the inner fission barrier

3.1. Comparison of different pairing schemes

The height of the fission barrier depends on the pairing. This is a well known fact from the early work of Ref. [41] where it was shown for reflection symmetric shapes that barrier heights decrease with increasing nuclear pairing. The study of the fission barrier in ^{240}Pu within the RMF+BCS framework of Ref. [42] showed that the enhancement of the pairing strength of the zero-range pairing force by 20% decreases the fission barrier by approximately 2 MeV. Similar results were obtained also in non-relativistic HFB calculations based on the Skyrme forces in Ref. [18]: the reduction of the pairing strength of zero-range pairing forces by approximately 15% leads to an increase of the fission barriers by roughly 2 MeV in the Actinides and can enhance it by up to 4 MeV in superheavy nuclei thus doubling the barrier heights. The impact of pairing on fission barriers has also been studied in the Skyrme+HF+BCS approach using a seniority pairing force and zero-range δ -interactions with different forms of density dependence in Ref. [20].

In Fig. 1 we investigate as a typical example the inner fission barrier of the nucleus ^{240}Pu first by RMF+BCS and then by full RHB calculations with four different pairing schemes. The major goal of this figure is to show the dependence of the potential energy surface (PES) and its profile on the pairing strength as a function of the deformation. Therefore we introduce a scaling factor g which allows us to change the strength of the pairing correlations in an appropriate way. Details will be discussed below. Note that we have not tried to adjust the pairing strengths in all these pairing schemes. As a result, the PES of the different panels of Fig. 1 cannot be compared directly.

Figs. 1a and b show RMF+BCS calculations with constant gap and with constant G within a pairing window of $E_{\text{cut-off}} =$

60 MeV. In the first case shown in Fig. 1a we use the same constant gap parameters Δ_τ for the entire deformation range. The size of this pairing gap parameters is determined for the ground state in the first minimum by a prescription given in Ref. [43]

$$\Delta_n = \frac{4.8}{N^{1/3}} \text{ MeV}, \quad \Delta_p = \frac{4.8}{Z^{1/3}} \text{ MeV}. \quad (12)$$

In order to see how the barrier depends in this case on the gap parameter we multiply this choice for the gap parameter with a scaling factor g

$$\Delta_\tau \rightarrow g\Delta_\tau \quad (13)$$

in the range between $g = 0.8$ and $g = 1.2$ in a step of 0.1. The different potential energy surfaces obtained in this way are normalized at the ground state. We observe only small changes of the barrier for the different values of g . The height of the barrier is the largest for the reduced gap with $g = 0.8$ and it drops only slightly with increasing pairing correlations.

In Fig. 1b we show results of similar calculations, but now with constant G . We start in the first minimum with the same values for the gap parameters as in Fig. 1a and determine in a self-consistent way for each value of g the strength parameters

$$G_\tau = \Delta_\tau / \sum_k u_k v_k \quad (14)$$

In a calculation with constant G this choice leads in the first minimum of Fig. 1b to the same gap parameters Δ_τ as in Fig. 1a. Of course, we also could have scaled the strength parameters $G_\tau \rightarrow gG_\tau$ directly. However, because of the strong non-linearity of the gap equation this leads to dramatic changes in the potential energy surfaces and the two calculations with constant gap and constant G would have been hard to compare. Therefore in Fig. 1b we compare the potential energy surfaces obtained from constant G -calculations using G_τ -values derived according to Eq. (14) after a self-consistent solution for the various scaled gap parameters. In this case the calculations for the various g -values in the first minimum are identical in Fig. 1a and Fig. 1b. However, the remaining part of the energy surfaces are very different. In particular the height of the barrier is now reduced by nearly a factor 2 and the relative changes for the various g -values are larger than in the case of constant gap.

This behavior can be understood by the fact that the minima and maxima (saddle points) along the fission path are induced by shell effects. The microscopic mechanism of this process is related to the density of the single-particle states in the vicinity of the Fermi level which is a function of the deformation [44, 45]. In Fig. 2 we show Nilsson diagrams for protons and neutrons in the nucleus ^{240}Pu . Minima in the potential energy surfaces are stable configurations. They corresponds to a region of low level density, whereas a saddle point occurs in the vicinity of level crossings, a region of higher level density. In regions of high level density it is easier for the quasi-particles to spread around the Fermi surface and therefore the size of the pairing correlations depends strongly on the level density. As a consequence we find a relatively small pairing gap at the minima of the PES and large pairing at the saddle points. Of course,

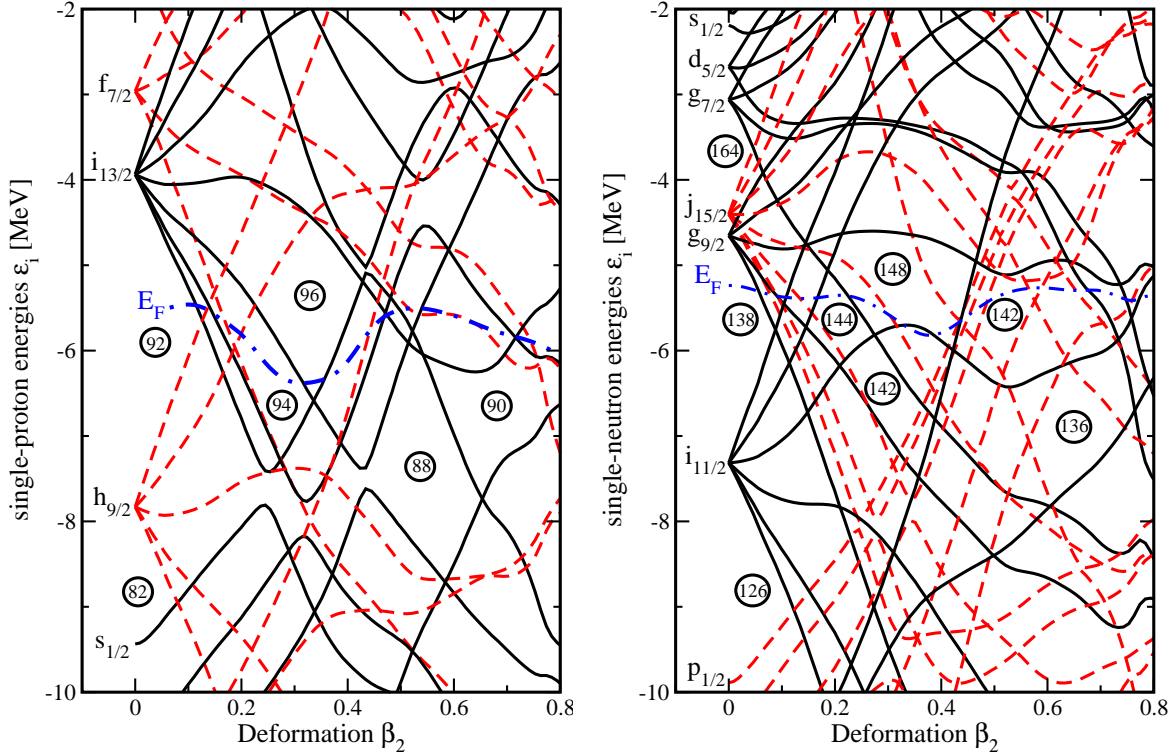


Figure 2: Proton and neutron single-particle energies in ^{240}Pu as a function of the quadrupole deformation β_2 . They are obtained in the RMF+BCS calculations with constant gap approximation and the NL3 parameterization of the RMF Lagrangian. Solid and dashed lines are used for positive and negative parity states, respectively.

this effect is restricted to the cases where we determine the gap in a self-consistent way using a pairing interaction, which does not change along the fission path.

Pairing correlations with partial occupations of the different levels in the neighborhood of the Fermi surface have the tendency to wash out shell effects and by this general argument we expect a reduction of the barrier height with increasing pairing correlations. In fact, we observe this tendency in all four panels of Fig. 1. However the gap at the Fermi surface is relatively small in nuclei (roughly 1 MeV) as compared to the shell effects which are of the order of $1\hbar\omega_0$ (≈ 5.6 MeV in ^{240}Pu). Thus we can understand that in the case of constant gap in Fig. 1a a variation of the scaling factor g in the range of 20% has almost no impact on the PES. This is a new result not available in the literature. Note that the constant gap approximation has been used in early RMF studies (Refs. [23, 24, 46]). In view of the results of the present analysis such investigations have to be treated with care. On the other hand the calculations with

constant G shown in Fig. 1b lead to oscillations of the gap parameters along the fission path (see Table 1).

The dramatic change of the fission barrier heights is not caused in the first place by the change of pairing correlations in total, but rather by the fact that the pairing correlations change along the fission path. To elaborate more on this oscillating behavior of pairing correlations we show in Fig. 3 the pairing energies E_{pair} defined in Eq. (8) for self-consistent calculations with the finite range Gogny-force D1S in the pairing channel. We find that these quantities are larger at the saddle point than at the normal deformed (ND) minimum. With increasing g , the magnitudes of the pairing energies at the saddle point grow faster than the ones at ND minimum. As a consequence, additional binding due to pairing (which is related to the pairing energies in a highly non-linear way) grows faster at the saddle point than at ND minimum with increasing g and as a result, the fission barrier becomes lower with increasing g . Note, however, that the dramatic changes in the pairing energy cannot be seen directly in the change of the barrier height, because they are compensated to some extent by the fact that larger pairing causes a wider distribution of the occupation probabilities v_k^2 around the Fermi surface.

In Figs. 1c and 1d we show potential energy surfaces obtained from self-consistent RHB calculations based on the parameter set NL3 using the Gogny D1S of Eq. (9) and the zero range δ -force of Eq. (10) in the pairing channel. For the δ -force we use the strength parameter $V_0 = 300$ MeV \cdot fm 3 and a pairing window of $E_{\text{cut-off}} = 60$ MeV. In both cases we introduce a

Table 1: Gap parameters for neutron and protons for several deformations along the fission path obtained by calculations with constant $G_n = 0.0399$ MeV and $G_p = 0.0616$ MeV, i.e. for the full black curve in Fig. 1b.

	$\beta = 0$	ND minimum	saddle point	SD minimum
Δ_n	1.560	0.912	1.335	1.033
Δ_p	1.280	1.056	1.535	1.236

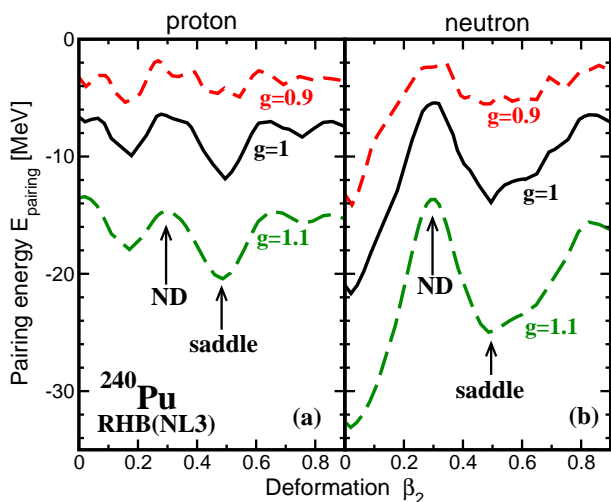


Figure 3: (Color online) Proton and neutron pairing energies in ^{240}Pu as functions of β_2 -deformation. They are obtained in the RHB calculations with the Gogny D1S force for indicated values of g . The arrows show the positions of the ND minimum and saddle point.

scaling parameter of the pairing interaction

$$V^{\text{PP}}(1,2) \rightarrow gV^{\text{PP}}(1,2) \quad (15)$$

and compare in this way the influence of the strength of the pairing force on the fission barrier. In both cases we observe a considerable reduction of the barrier height with increasing g -values. This has the same origin as in the case of the constant G calculations in Fig. 1b. Note, however, that we cannot compare directly these results with those of Fig. 1b, because we do not scale the strength parameters G_τ of the seniority force by the factor g but rather the resulting gap parameters Δ_τ of Fig. 1a. This leads to much smaller changes of the parameters G_τ .

Summarizing the results of this section we observe for all pairing models in Fig. 1 variations of the PES with pairing. Increasing pairing leads to a reduction of the barrier height. This effect is, however, relatively small for calculations with constant gap. On the other hand for self-consistent calculations the oscillations in the level density at the Fermi surface induce pronounced changes of pairing along the fission path and a considerable reduction of the barrier heights with increasing strength of the effective interaction in the pairing channel.

3.2. Finite versus zero range pairing

The basic advantage of the Gogny force is its finite range, which automatically guarantees a proper cut-off in momentum space [47]. Calculations with interactions of finite range require a substantial numerical effort and therefore many modern energy density functionals like Skyrme functionals are based on forces with zero range. In the ph -channel, where either only the levels up to the Fermi surface are occupied or where the analytical form of the occupation numbers v_k^2 in Eq. (1) leads to a fast convergence in momentum space, a gradient expansion of finite range interactions leading to zero-range forces of the Skyrme type [48] are well justified and successful. This is no

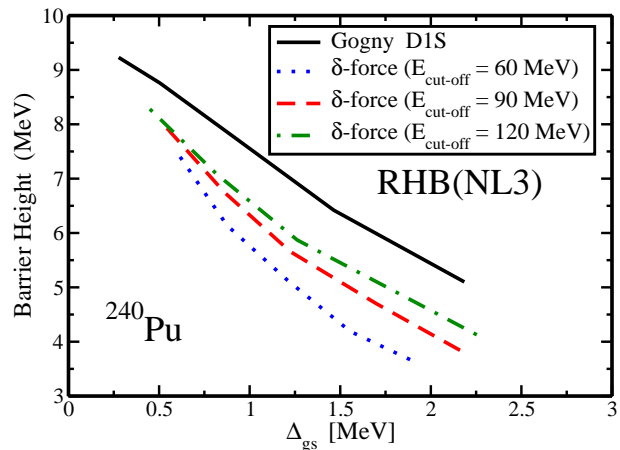


Figure 4: (Color online) The dependence of the fission barrier height on the pairing gap in the ground state shown for the RHB calculations with Gogny D1S force and δ -force. The results for δ -force are displayed for 3 different values of the cut-off energy $E_{\text{cut-off}}$.

longer true in the pp -channel, where the analytical form of the factors $u_k v_k$ in the pairing tensor κ includes high momenta and leads to a ultra-violet divergence. The same is true for the seniority pairing which can be considered as the $J = 0$ part of the surface delta interaction [28]. In all these cases one is forced to use a cut-off energy $E_{\text{cut-off}}$ in order to avoid divergencies.

The strength parameters of the pairing force V_0 (or G) are usually deduced for a fixed value of the cut-off energy $E_{\text{cut-off}}$ from the pairing gaps Δ extracted from experimental data such as the odd-even mass differences at the ground state in the ND minimum and it is assumed that the strength parameters do not depend on the nuclear deformation. Thus, it is interesting to see how the description of the fission barriers differs in the RHB calculations with zero range and with finite range pairing forces under the condition that the pairing strength parameters are defined by the same set of experimental data at the normal-deformed minimum. In particular we will investigate whether the barrier depends on the choice of the cut-off energy in the case of zero range pairing forces.

In Fig. 4 we study the dependence of the height of the fission barrier in the nucleus ^{240}Pu on the size of pairing correlations in the ground state of the ND minimum. For this purpose we carry out RHB calculations with the Gogny force D1S and a zero-range δ -force in the pairing channel for various values of the scaling parameter g in Eq. (15). The resulting barrier height is plotted as a function of the resulting average pairing gap (11) in the ground state $\Delta_{\text{gs}} = \frac{1}{2}(\langle\Delta\rangle_n + \langle\Delta\rangle_p)$. The full (black) curve shows the results obtained with the Gogny force D1S and the other three lines correspond to calculations with the zero range δ -force in Eq. (10) using different cut-off energies $E_{\text{cut-off}} = 60, 90, \text{ and } 120$ MeV. This figure clearly indicates that there is a strong dependence of the fission barrier height on the treatment of pairing correlations. For the Gogny force D1S we find a nearly linear decrease of the fission barrier height by roughly 1.00 MeV per 0.4 MeV change in the gap Δ_{gs} . For the same value of Δ_{gs} the fission barrier is smaller in the calculations with zero range force as compared with the ones based on the D1S

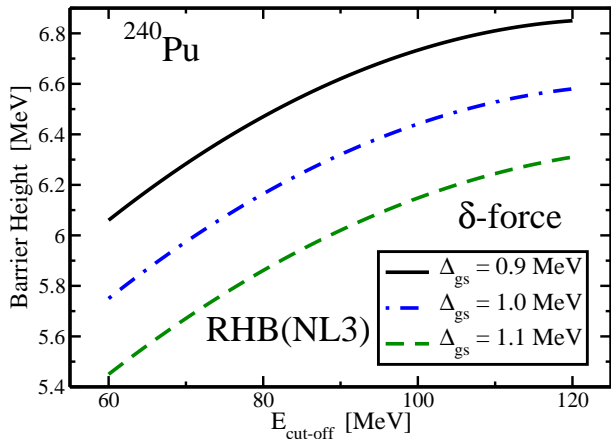


Figure 5: (Color online) The dependence of the fission barrier on the cut-off energy $E_{\text{cut-off}}$ in the RHB calculations with δ -force given for 3 different values of pairing gap Δ_{gs} in the normal-deformed ground state.

Gogny force. Again we see a decreasing barrier height with increasing Δ_{gs} . However, in the case of zero range force the results also depend on the cut-off energy $E_{\text{cut-off}}$. Only for very small pairing correlations $\Delta_{\text{gs}} \approx 0.5$ MeV we have more or less the same barrier heights in the calculations with zero range. For larger pairing we observe increasing differences between barrier heights calculated with the various values of $E_{\text{cut-off}}$.

In particular, for small cut-off energies we find considerably lower fission barriers than those obtained with the finite range Gogny force. This is shown in detail in Fig. 5 where for the same calculations the height of the fission barrier is plotted as a function of the cut-off energy $E_{\text{cut-off}}$ for three values of the gap parameter in the ground state ($\Delta_{\text{gs}} = 0.9, 1.0,$ and 1.1). The dependence of the barrier height on the cut-off energy is not eliminated even for these large values of $E_{\text{cut-off}}$ which are much larger than the typical ones used in many calculations with δ -force (see, for example, Ref. [18]).

3.3. Extrapolation to superheavy nuclei

Systematic experimental spectroscopic data, such as odd-even mass differences and the moments of inertia, which allow to extract the information on the strength of pairing correlations are available only up to the proton number $Z \approx 102$ and neutron number $N \approx 158$. With increasing proton and neutron numbers such data become scarce and less reliable. Thus, existing predictions for superheavy nuclei centered around $Z = 120$ and 126 are based on drastic extrapolations involving the changes of proton number by more than 20 particles and neutron numbers by 14-26 particles. As with any extrapolation there is a considerable degree of uncertainty, and modifications of the strength of the pairing interaction by $\pm 10\%$ cannot be ruled out. Indeed, while providing the average description of pairing properties modern pairing forces show sometimes appreciable local deviations from experiment for physical observables which are strongly affected by pairing (see, for example, Fig. 1 in Ref. [42] and Ref. [49]).

Fig. 6 shows that modifications of the strength of the pairing interaction by $\pm 10\%$ have a profound effect on properties

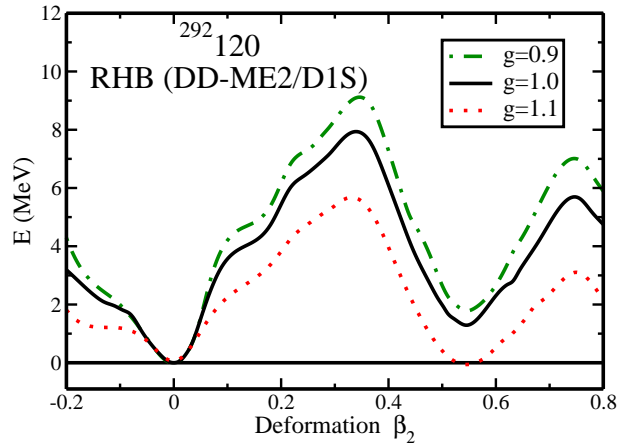


Figure 6: (Color online) Potential energy surfaces in the $Z = 120, N = 172$ nucleus obtained in the RHB calculations with the DD-ME2 parameterization of the RMF Lagrangian and different values of the scaling factor g .

of superheavy nuclei. For example, a decrease of this strength by 10% (the $g = 0.9$ curve in Fig. 6) increases the inner fission barrier by ≈ 1.0 MeV, and thus increases the stability of this nucleus against fission considerably. On the contrary, the increase of the strength of the pairing force by $\sim 10\%$ will modify the situation drastically (the $g = 1.1$ curve in Fig. 6). Indeed, we find in this case that the superdeformed minimum becomes lower than the spherical minimum. This could indicate that the spherical minimum would no longer be the ground state of the system since the superdeformed minimum is lower in energy. However, one should remember that odd-multipole deformations (not included in the current calculations) are important at the outer fission barrier, and thus if included they will most likely eliminate this barrier [17]. As a consequence the second minimum will not really stay as a minimum in the PES. In this situation, the ground state in the spherical minimum is stabilized only by the inner fission barrier of the ≈ 5 MeV height.

4. Fission barriers in Actinides and superheavy nuclei

In Figs. 7 and 8 we compare the results of RHB calculations with the parameter sets NL3 [50] and DD-ME2 [51] of the RMF Lagrangian with available experimental data on the heights of the inner fission barrier in Actinides and superheavy nuclei. In these calculations the original Gogny force is used (scaling factor $g = 1.0$). It was tested that with this value of g the moments of inertia of even-even nuclei, which are very sensitive to the strength of pairing correlations, are reasonably well described in cranked RHB calculations with the NL3 force in the Nobelium region [52] and in the lighter Actinide nuclei [53].

Fig. 7 compares the calculated heights E of the inner barrier with experiments for Actinide nuclei. While the dependence of E on the neutron number N is reasonably well described in both parameterizations, the dependence on the proton number Z is not reproduced. The calculated values of E increase with increasing Z while the experimental inner barriers almost do not depend on Z . The inner fission barriers obtained in the cal-

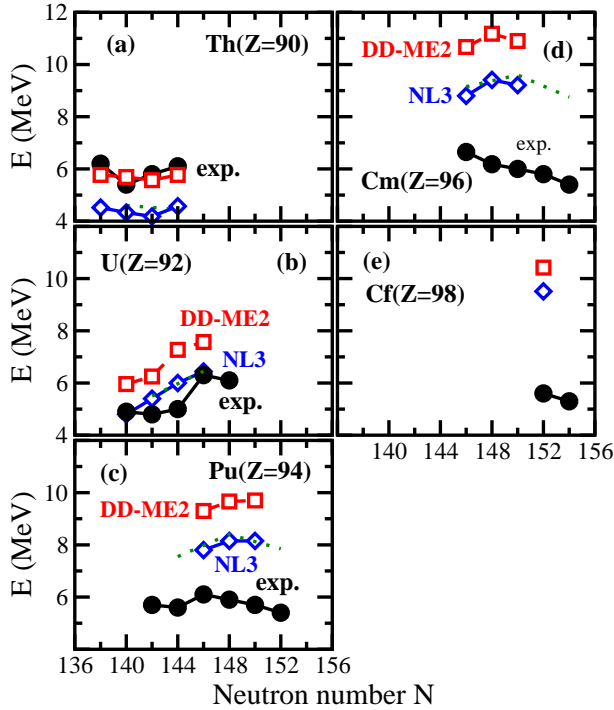


Figure 7: (Color online) Experimental and calculated heights of the inner fission barriers in Actinide nuclei. Experimental data are taken from Table IV in Ref. [18]. A typical uncertainty in the experimental values, as suggested by the differences among various compilations, is of the order of ± 0.5 MeV [18]. Results of RHB calculations with the parameter sets NL3 and DD-ME2 of the RMF Lagrangian are presented. The dotted lines show the results of the RMF+BCS calculations of Ref. [17] which are performed in steps of $\Delta N = 4$.

culations with the DD-ME2 parameterization exceed the ones obtained with the NL3 parameterization by 1-2 MeV.

Fig. 8 clearly shows that the fission barriers in superheavy nuclei are well described in the RHB calculations with the DD-ME2 parameterization. The calculated barrier heights are either close to the experimental lower limit or slightly exceed it. Only in the case of the ($Z = 114, N = 176$) system, the calculated fission barrier is slightly below the experimental value. However, considering the expected error bars on the height of the fission barrier this fact is not important. On the contrary, the results of the RHB calculations with the NL3 force considerably (by ~ 2 MeV) underestimate the height of the fission barriers.

The RHB results obtained with the NL3 force are very close to the ones obtained earlier in the RMF+BCS framework with the same NL3 force in Ref. [17], see Fig. 7 and Fig. 8. They are typically within 0.5 MeV of each other. The RMF+BCS barriers of Ref. [17] are either very close to the RHB barriers or slightly higher (by several hundreds keV) in the Actinide nuclei. On the contrary, they are lower by 0.5-0.8 MeV than the RHB barriers in superheavy nuclei. Thus, in going from Actinides to superheavy nuclei, the change in the height of the fission barriers is more pronounced (by ≈ 1 MeV) in the RMF+BCS framework as compared with the RHB.

Based on the RHB results, one can conclude that the calculations based on the NL3 parameterization do not leave the room for triaxiality and the correlations beyond mean field; this con-

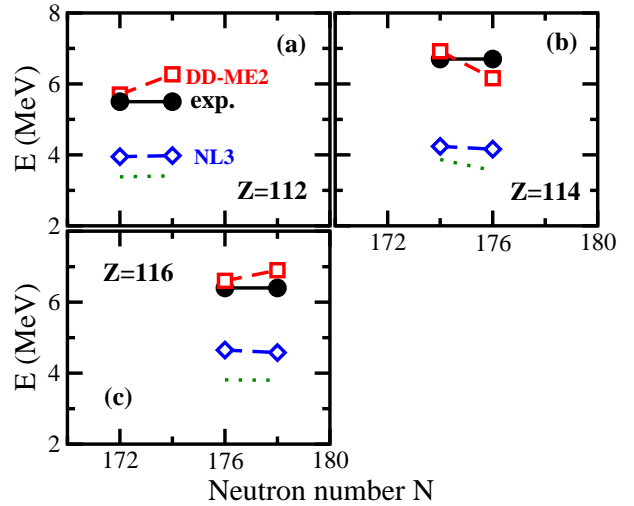


Figure 8: (Color online) The same as in Fig. 7, but for superheavy nuclei. Experimental data, which specifies the lower limit of the heights of fission barriers, are taken from Ref. [2]. The assignment of the neutron number has some uncertainty, therefore, the same experimental barrier appears for the nuclei with the same proton number Z .

Table 2: Excitation energies E (in MeV) of fission isomers as obtained in the RHB calculations with the Gogny D1S force and indicated parameterizations of the RMF Lagrangian. Last column shows experimental data taken from Ref. [54].

Nucleus	$E(\text{NL3})$	$E(\text{DD-ME2})$	$E(\text{exp})$
^{236}U	1.72	2.24	2.75
^{238}U	1.70	1.54	2.557
^{240}Pu	2.29	2.21	~ 2.8

clusion is consistent with the one obtained in the RMF+BCS framework earlier [17]. The RHB+NL3 calculations underestimate the experimental fission barriers in some nuclei already on the mean field level. As discussed in the introduction, the triaxiality can lower the fission barriers by up to 3 MeV or sometimes even by larger amount. In addition, the correlations beyond mean field can lower fission barrier by as much as 1 MeV [17] (see also Ref. [9]). It is reasonable to expect that with these degrees of freedom included the majority of the results with the NL3 force will fall below the experiment. On the contrary, the experimental fission barriers are overestimated in the RHB calculations with DD-ME2 force which indicates that there is sufficient room for triaxiality and the correlations beyond mean field. It is also interesting to mention that the heights of fission barriers as obtained with the density-dependent DD-ME2 force are close to the typical values obtained in the calculations with Skyrme force [17]. On the contrary, the NL3 parameterization of the RMF Lagrangian, which has no density dependence in the isovector channel, systematically predicts lower barriers than most Skyrme forces [17].

An additional constraint on the selection of the force may be provided by the energy of the 0^+ fission isomeric state. It turns out that for Actinides this energy is less dependent on the

variation of the pairing strength than the height of the fission barrier (see Fig. 1) thus providing a more robust probe. Reliable values for the energies of the fission isomers in even-even nuclei are available only for three nuclei (see Table 2). It turns out that in average the NL3 and DD-ME2 parameterizations of the RMF Lagrangian provide similar results for the energies of the fission isomers: these energies are underestimated by at least 0.5 MeV.

5. Conclusions

The current investigation of fission barriers within covariant density functional theory clearly indicates that when aiming at a quantitative understanding of fission properties of heavy and superheavy elements, it is important to keep the pairing channel under control. It shows that the frequently used constant gap approximation provides unphysical results for the height of fission barrier. On the contrary, the constant strength approximation shows a similar functional dependence of the height and the shape of barrier as the RHB approach. Therefore it is important to treat the pairing properties in a self-consistent way.

Seniority forces or zero range forces depend at least on two parameters, the strength and the cut-off energy. They are usually adjusted to the experimental pairing properties in the ground state for a fixed value of the cut-off energy. It is shown that this procedure leaves room for uncertainties in the fission barriers of up to 1 MeV.

The extrapolation to superheavy nuclei leads to some uncertainties in the definition of the pairing strength in the $Z = 120$ and 126 regions of superheavy nuclei. It was shown that 10% uncertainties in the pairing strength have drastic consequences for the structure of these superheavy nuclei.

The DD-ME2 force is the only presently known parameterization of the RMF Lagrangian which provides a good description of fission barriers in superheavy nuclei in axially symmetric calculations. Previous and current studies within covariant density functional theory show that other RMF forces either considerably underestimate the barriers or do not leave the room for the triaxiality at the saddle point.

ACKNOWLEDGEMENTS

This work has been supported by the U.S. Department of Energy under the grant DE-FG02-07ER41459, by the Bundesministerium für Bildung und Forschung (BMBF), Germany, under Project 06 MT 246, by the DFG cluster of excellence “Origin and Structure of the Universe” (www.universe-cluster.de), and by the Hellenic State Scholarship foundation (IKY).

References

- [1] A. Sobiczewski and K. Pomorski, Prog. Part. Nucl. Phys. **58**, 292 (2007).
- [2] M. G. Itkis, Y. T. Oganessian, and V. I. Zagrebaev, Phys. Rev. **C65**, 044602 (2002).
- [3] J. Dudek *et al.*, Eur. Phys. J. **A20**, 15 (2004).
- [4] A. V. Afanasjev and H. Abusara, Phys. Rev. **C78**, 014315 (2008).
- [5] M. Arnould and K. Takahashi, Rep. Prog. Phys. **62**, 395 (1999).
- [6] A. Mamdouh, J. M. Pearson, M. Rayet, and F. Tondeur, Nucl. Phys. **A679**, 337 (2001).
- [7] M. Brack, J. Damgaard, A. S. Jensen, H. C. Pauli, V. M. Strutinsky, and C. Y. Wong, Rev. Mod. Phys. **44**, 320 (1972).
- [8] A. Baran, K. Pomorski, A. Lukasiak, and A. Sobiczewski, Nucl. Phys. **A361**, 82 (1981).
- [9] R. A. Gherghescu, J. Skalski, Z. Patyk, and A. Sobiczewski, Nucl. Phys. **A651**, 237 (1999).
- [10] P. Møller, A. J. Sierk, and A. Iwamoto, Phys. Rev. Lett. **92**, 072501 (2004).
- [11] I. Muntian and A. Sobiczewski, Acta Phys. Pol. **B36**, 1359 (2005).
- [12] P. Møller, A. Sierk, T. Ichikawa, A. Iwamoto, R. Bengtsson, H. Uhrenholt, and S. Åberg, J. Phys. **G36**, 013101 (2009).
- [13] H. Flocard, P. Quentin, D. Vautherin, M. Veneroni, and A. K. Kerman, Nucl. Phys. **A231**, 176 (1974).
- [14] C. Guet, H.-B. Hakansson, and M. Brack, Phys. Lett. **B97**, 7 (1980).
- [15] M. Bender, K. Rutz, P.-G. Reinhard, J. A. Maruhn, and W. Greiner, Phys. Rev. **C58**, 2126 (1998).
- [16] M. Bender, K. Rutz, P.-G. Reinhard, and J. A. Maruhn, Euro. Phys. J. **A7**, 467 (2000).
- [17] T. Bürvenich, M. Bender, J. A. Maruhn, and P.-G. Reinhard, Phys. Rev. **C69**, 014307 (2004).
- [18] S. G. M. Samyn and J. M. Pearson, Phys. Rev. **C72**, 044316 (2005).
- [19] A. Sobiczewski and M. Kowal, Phys. Scripta **T125**, 68 (2006).
- [20] A. Staszczak, J. Dobaczewski, and W. Nazarewicz, Int. J. Mod. Phys. **E16**, 310 (2007).
- [21] J. F. Berger, M. Girod, and D. Gogny, Nucl. Phys. **A428**, 23c (1984).
- [22] M. Warda, J. L. Egido, L. M. Robledo, and K. Pomorski, Phys. Rev. **C66**, 014310 (2002).
- [23] V. Blum, J. Maruhn, P.-G. Reinhard, and W. Greiner, Phys. Lett. **B323**, 262 (1994).
- [24] K. Rutz, J. A. Maruhn, P.-G. Reinhard, and W. Greiner, Nucl. Phys. **A590**, 680 (1995).
- [25] S. Ćwiok, J. Dobaczewski, P.-H. Heenen, P. Magierski, and W. Nazarewicz, Nucl. Phys. **A611**, 211 (1996).
- [26] D. Vautherin, Phys. Rev. **C7**, 296 (1973).
- [27] Y. K. Gambhir, P. Ring, and A. Thimet, Ann. Phys. (N.Y.) **198**, 132 (1990).
- [28] P. Ring and P. Schuck, *The Nuclear Many-Body Problem* (Springer-Verlag, Berlin, 1980).
- [29] H. Kucharek and P. Ring, Z. Phys. **A339**, 23 (1991).
- [30] P. Ring, Prog. Part. Nucl. Phys. **37**, 193 (1996).
- [31] J. Dechargé and D. Gogny, Phys. Rev. **C21**, 1568 (1980).
- [32] F. Chappert, Phd thesis, Université de Paris sud (unpublished), 2007.
- [33] A. Bulgac, Phys. Rev. **C65**, 051305(R) (2002).
- [34] J. F. Berger, M. Girod, and D. Gogny, Comp. Phys. Comm. **63**, 365 (1991).
- [35] J. L. Egido and L. Robledo, Nucl. Phys. **A494**, 85 (1989).
- [36] A. Valor, J. L. Egido, and L. M. Robledo, Phys. Lett **B392**, 249 (1997).
- [37] T. Gonzales-Llarena, J. L. Egido, G. A. Lalazissis, and P. Ring, Phys. Lett. **B379**, 13 (1996).
- [38] A. V. Afanasjev, J. König, and P. Ring, Phys. Rev. **C60**, 051303(R) (1999).
- [39] D. Vretenar, A. V. Afanasjev, G. A. Lalazissis, and P. Ring, Phys. Rep. **409**, 101 (2005).
- [40] P. Ring, Y. K. Gambhir, and G. A. Lalazissis, Comp. Phys. Commun. **105**, 77 (1997).
- [41] W. Stepień and Z. Szymanski, Phys. Lett. **B26**, 181 (1968).
- [42] K. Rutz *et al.*, Phys. Lett. **B468**, 1 (1999).
- [43] P. Møller and J. Nix, Nucl. Phys. **A536**, 20 (1992).
- [44] V. M. Strutinsky, Nucl. Phys. **A95**, 420 (1967), a122 (1968) 1.
- [45] V. M. Strutinsky, Nucl. Phys. **A122**, 1 (1968).
- [46] Z. Ren, F. Tai, and D.-H. Chen, Phys. Rev. **C66**, 064306 (2002).
- [47] J. F. Berger, M. Girod, and D. Gogny, Comp. Phys. Comm. **61**, 365 (1991).
- [48] J. W. Negele and D. Vautherin, Nucl. Phys. **A207**, 298 (1973).
- [49] S. Hilaire *et al.*, Phys. Lett. **B531**, 61 (2002).
- [50] G. A. Lalazissis, J. König, and P. Ring, Phys. Rev. **C55**, 540 (1997).
- [51] G. A. Lalazissis, T. Nikšić, D. Vretenar, and P. Ring, Phys. Rev. **C71**, 024312 (2005).
- [52] A. V. Afanasjev, T. L. Khoo, S. Frauendorf, G. A. Lalazissis, and I. Ahmad, Phys. Rev. **C67**, 024309 (2003).
- [53] A. Afanasjev, un-published.
- [54] B. S. R. Zywina and R. B. Firestone, Nucl. Data Sheets. **A241**, 241 (2002).